SLAC-PUB-11019

CHERENKOV IMAGING TECHNIQUES FOR THE FUTURE HIGH LUMINOSITY MACHINES*

J. VA'VRA†
Stanford Linear Accelerator Center, 2575 Sand Hill Road, Menlo Park, CA 94025, USA,tel. 650-926-2658, jjv@slac.stanford.edu

The paper discusses Cherenkov Ring Imaging detectors for use in future high luminosity colliders, such as B-factories, or hadron machines, such as the Eloisatron.

1. Introduction

What is a future of the Cherenkov Ring Imaging technique, say in 10-15 years? There are several experiments, which are either already or will be soon producing B physics: BaBar, Belle, CDF, LHC-b and BTeV. In addition, there is some chance that either Super-BaBar or Super-Belle would be built, and will push the B-physics up to luminosities 10^{35}-10^{36} $cm^{-2}sec^{-1}$. Therefore, it is very likely that most of the B-physics questions will be well answered by the year ~2015.

All above mentioned detectors, except CDF, have the particle identification (PID) based on the RICH concept. On the other hand, the Linear Collider (LC) detectors plan to use a dE/dx PID technique. This is because the goal is to discover the Higgs boson and the Super Symmetric particles, where tracking and calorimetry is believed to be more important. The motivation to reach even higher energies, such as those available at the cancelled SSC, i.e., to build the Eloisatron, would increase if LHC does not discover the Higgs or the Super Symmetric particles.

The motivation to employ the RICH PID technique in future accelerators would increase if new heavy particles, for example quark molecules, are discovered as one increases the CMS energy. There would be a need to understand their decay products in order to assign their quantum numbers, and sort out the expected and unexpected. The Cherenkov technique would be the only PID method available as the decay products would have very likely high momentum.

In this paper we want to limit the discussion of the new Cherenkov techniques to three major areas:

* Work supported in part by the Department of Energy, contract DE-AC02-76SF00515
† Work partially supported by grant 2-4570.5 of the Swiss National Science Foundation.

Presented at the INFN Eloisatron Project: 42nd Workshop on Innovative Detectors for Supercolliders, 9/28/2003 - 10/4/2003, Erice, Sicily, Italy

- RICH operating in a 4π-detector, such as is needed for the B-physics, with a PID capability that reaches a momentum of 4-6 GeV/c. Examples are Super BaBar or Super Belle proposals, which are discussing to build a Focusing DIRC or a TOP counter. These detectors use a very small radial size to limit the size of the calorimeter. This means to use solid radiators, such as Fused silica. To enhance the performance, there is an R&D in progress to correct the chromatic error by timing, and use highly pixilated detectors capable of operating in a magnetic field of 1.5 Tesla. To correct the chromatic error by timing requires a resolution in the range of 50-100ps per single photon, and this requires to introduce new techniques.
- RICH operating in a 4π-detector and with a PID capability that reaches a momentum range of 10-40 GeV/c, which is similar to that of the SLD CRID or DELPHI RICH detectors, are most difficult technologically. To embark on such an R&D program could be motivated by a discovery of a heavy new particle on the same scale as the Z boson.
- Fixed target experiments use a well established RICH methodology by now, thanks to experiments such as HERA-B, COMPASS or ALICE, and therefore we will limit their discussion to a minimum. Examples of new experiments are LHC-b and B-TeV.

2. "DIRC-like" detectors

The DIRC[1] concept basically uses a "pinhole" geometry, where the bar's exit area, together with a photon detecting pixel position, define the photon exit angles in 2D; the time and the track position defines the third coordinate. The concept was invented by B. Ratcliff [1]. The principle of BaBar DIRC, the first among the DIRC-like detectors, is shown in Fig. 1a. To determine the Cherenkov angle θ_c, one measures a track position, a time-of-propagation (TOP), and Δz and Δr. This over-determines the triangle and therefore two measurements are sufficient in theory. In practice it is a good idea to measure all three variables to have a redundancy against background and ambiguities. In the present BaBar DIRC, the time measurement is not good enough to determine the Cherenkov angle θ_c. The time is, however, used to reduce the background very successfully. The TOP variable is defined as $TOP(\Phi,\theta_c) = [L/v_g(\lambda)]q_z(\Phi,\theta_c)$, where θ_c is the Cherenkov angle, L is a distance of light travels in the bar, $v_g(\lambda)$ is a group velocity of light at wavelength λ, and $q_z(\Phi,\theta_c)$ is a z-component of the unit velocity vector. Figure 1b shows the most simple Cherenkov image formation in 2D plane using x&y coordinates. It is also possible to form the 2D image using two different variables, Φ (horizontal emission angle) & TOP (time-of-propagation), which is used in the TOP counter. In the Focusing DIRC, which is the next step after the BaBar DIRC,

[1] DIRC uses internally reflected Cherenkov light, which is opposite to the CRID detector at SLD, which used the transmitted Cherenkov light (therefore letters in two names are backward).

we want to use imaging using all three variables x&y&TOP. In addition, the TOP variable will be used to correct the chromatic error by timing, and, as is done in case of BaBar DIRC, to suppress the background.

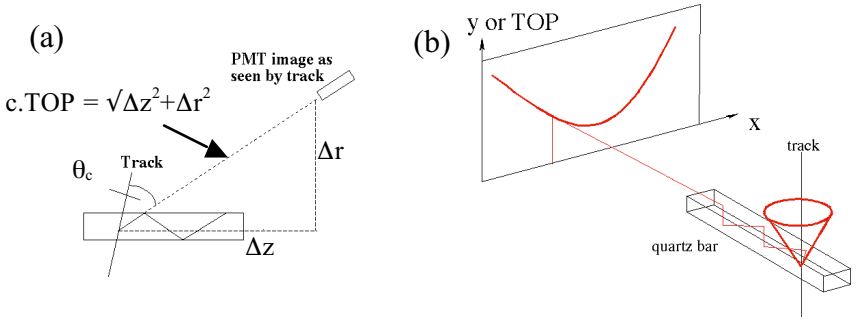

Figure 1. (a) To determine the Cherenkov angle θ_c, one measures a track position, a photon time-of-propagation (TOP), Δz and Δr. This over-determines the triangle. (b) The Cherenkov Ring image can be then displayed on a screen. The optics uses a "pinhole" geometry, where bar's exit area, together with a photon detecting pixel position, define the photon exit angles in 2D. One can either display x&y (BaBar DIRC), or x&TOP (TOP counter), or x&y&TOP (Focusing DIRC).

2.1. *BaBar DIRC*

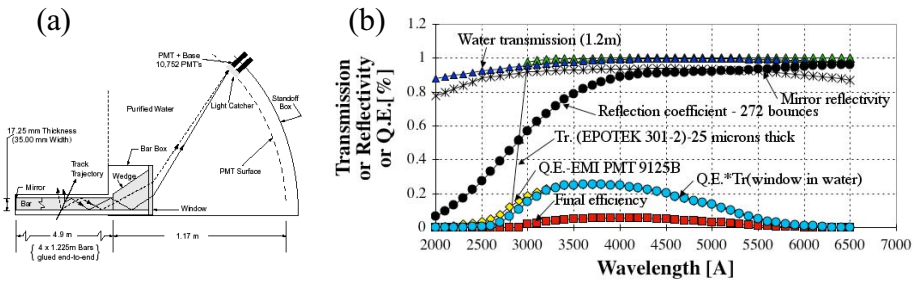

Figure 2. (a) DIRC RICH at BaBar [2]. (b) Various efficiencies or transmissions of the detector for track perpendicular to the bar.

Figure 2a shows its principle [2]. The resolution parameters are shown in Table 1, and the π/K separation performance in Fig. 9. The photon detector uses ~11,000 one-inch dia. EMI 9125B PMTs. The time resolution is determined to σ~1.6ns per single photon, which is good enough to reject the background, however, not good enough to correct the chromatic error by timing. The wavelength bandwidth of BaBar DIRC is shown in Fig. 2b. One can see that a crucial variable is the internal reflection coefficient of a Fused silica bar surface.

It was not obvious, at the time when DIRC was proposed, that this quantity will not cause a problem in a large size detector. One can also see that another critical variable, which is defining the bandwidth boundary, is the EPOTEK 301-2 optical glue used to glue fused silica bars together. In this paper we will not go into more detailed description of the entire DIRC R&D effort [3] , except to say that many tests were required to develop DIRC successfully. In the end, the DIRC detector proved itself as a very good PID performer, exactly matching BaBar needs, and providing exceptional stability [2].

2.2. *Focusing DIRC prototype*

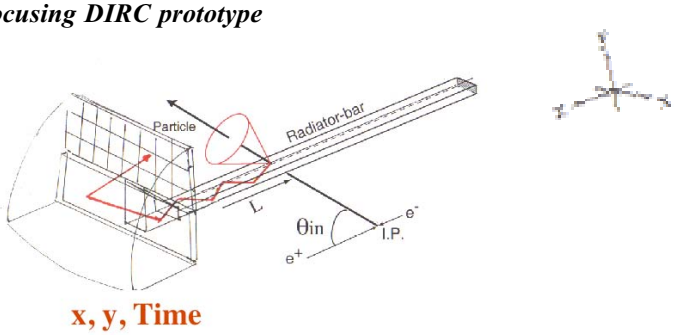

Figure 3. Optical concept of the Focusing DIRC, which measures x, y and time-of-propagation (TOP) for each Cherenkov photon. The time is measured with accuracy of σ~100ps, which is required to correct the chromatic error contribution to the Cherenkov angle by timing. The spherical mirror is used to remove optically the bar thickness from the resolution calculation.

Figure 3 shows a principle of imaging with the Focusing DIRC, which measures x, y and time-of-propagation (TOP) for each Cherenkov photon. The time needs to be measured to σ~100ps to be able to correct the chromatic error contribution by timing.

Figure 4 shows a practical realization of this idea, the so-called Focusing DIRC prototype. The main motivation to build it was to learn more about the photon detector suitable for this application, its electronics, and to develop methods for correcting the chromatic error by timing. A long ~3.7m long bar (equipped with a flat mirror at the far end), which was a leftover from the BaBar DIRC construction, is coupled to a fused silica bar block, which is placed in a large bar box containing the CRID spherical mirror with a radius of 97cm. The purpose of the spherical mirror is to optically remove the bar thickness from the resolution consideration. The mirrors focal plane is located on the outer surface of the bar box window, on which the photon detectors are placed. The free space in the bar box is filled with mineral oil [4] because its refraction index matches well the Fused silica index (see Fig. 5). However, its transmission is worse than that of water, or EPOTEK301-2 glue, which is used to glue the bars together

(see Fig. 6). However, we have not tried any purification of the mineral oil, which is incidentally necessary for water to be useable for the BaBar DIRC.

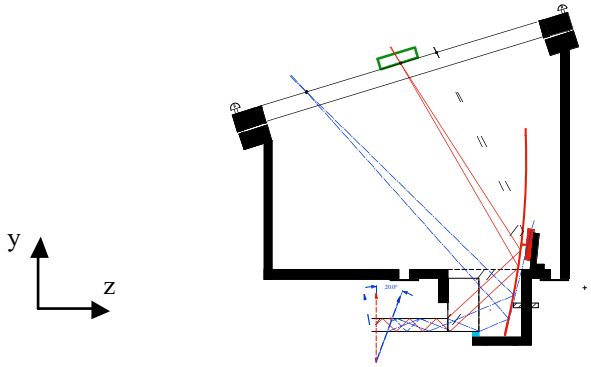

Figure 4. Optical design of the Focusing DIRC prototype. A bar is coupled to a bar box, filled with mineral oil for a good optical coupling. The bar box houses the CRID spherical mirror, which is used to remove the bar thickness from the resolution consideration. The photon detectors are placed in the focal plane. Picture is shown in a cut along the y-z plane (x axis points out of paper).

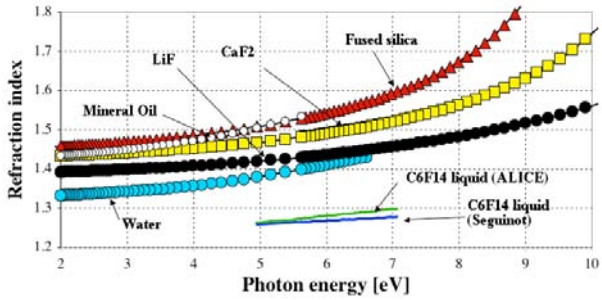

Figure 5. Refraction index of various solid and liquid materials as a function of photon energy. We plan to use the mineral oil [4] in the Focusing DIRC prototype because it has nearly perfect match to the index of Fused silica.

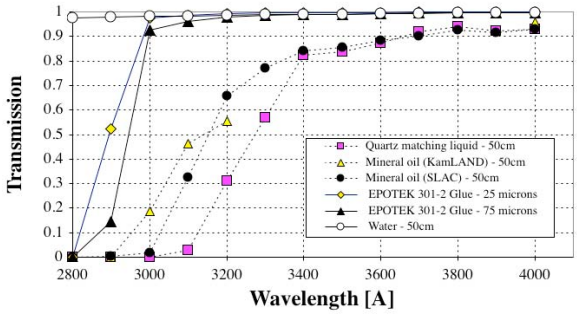

Figure 6. Transmission in 50cm of mineral oil [4] and the quartz matching liquid. This is compared to the transmission of 25&75 micron thick EPOTEK301-2 glue and 50cm of water. The quartz matching liquid has the worst transmission. The mineral oil (SLAC) was not purified, i.e., some further improvement is still possible.

To understand the effect of chromaticity on timing, it is best to consider only Cherenkov photons propagating in the y-z plane (see Fig.3). Figure 7 shows the chromatic time dispersion over the Bialkali photocathode bandwidth, if the track enters the bar perpendicularly either at the bar mirror end (~3.5m bar length), or the bar box end (~7m bar length for photons traveling towards the bar mirror and back). It is clear that any detector having a timing resolution of σ~100ps will easily calibrate this effect. What is less clear is how well one will be able to calibrate the chromaticity corresponding to different photon path lengths, different incident track angles, track positions within the bar, etc.

Figure 8 shows a difference in the TOP time for 4GeV/c pions and Kaons, if they would travel in the y-z plane along 3.5m long bar. One can see that a π/K time separation based on the single photons of the same color is much smaller at 4GeV/c than the overall time spread over the entire bandwidth. Figure 9 shows that one can introduce the chromatic cuts by slight rotation in the Θ_{track} angle, which may be useful to check the timing resolution limit.

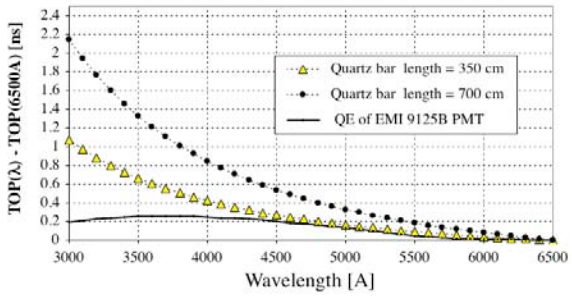

Figure 7. Time dispersion due to the chromaticity for two bar lengths, one for beam entering the far end of the bar, and one for beam entering the closest position to a detecting end. A 4GeV/c pion beam enters the bar perpendicularly. Photons propagate in y-z plane only. Solid curve shows the quantum efficiency of a typical Bialkali photocathode.

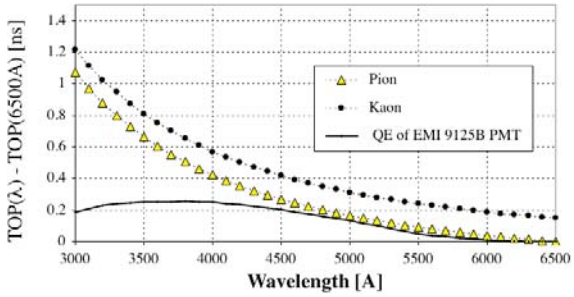

Figure 8. Time dispersion due to the chromaticity, or a time-of-propagation (TOP) of a Cherenkov photon as a function photon wavelength. A 4 GeV/c pion/Kaon enters the bar perpendicularly at a distance of 3.5 meters from the detector. Photons propagate in y-z plane only. Solid curve shows the quantum efficiency of a typical Bialkali photocathode.

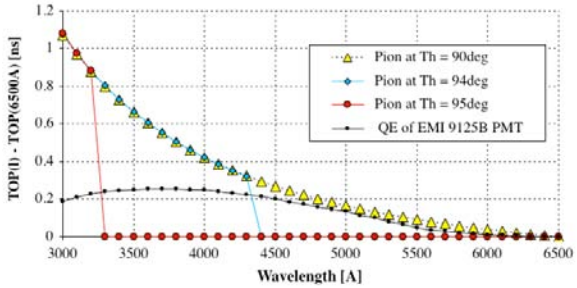

Figure 9. One can introduce chromatic cuts by a slight rotation of incident track angle relative to bar. The picture was generated for 10 GeV/c pion entering the bar with $\Theta_{track} = 90^o, 94^o$ and 95^o.

Table 1. Contributions to the Cherenkov angle resolution for the BaBar DIRC, the SLAC Focusing DIRC prototype and the "ultimate" DIRC of the future.

Contribution to Cherenkov angle resolution [mrads]	**Present BaBar DIRC**	**Focusing DIRC prototype**	**Ultimate DIRC of the future**
$\Delta\theta_{track}$	~1	~1	~1
$\Delta\theta_{chromatic}$	~5.4	~1	~1
$\Delta\theta_{transport\ along\ the\ bar}$	2-3	2-3	2-3
$\Delta\theta_{bar\ thickness}$	~4.1	~1	~1
$\Delta\theta_{PMT\ pixel\ size}$	~5.5	~4	~1
$\Delta\theta_c^{track}$	~2.4	~1.5	~1.0
Total $\Delta\theta_c^{photon}$	~9.6	~4.8	~3.3

Table 1 compares the expected contributions to the Cherenkov angular resolution of the Focusing DIRC prototype with that of the BaBar DIRC and the "ultimate" DIRC (see next chapter). It is assumed that the effective way to correct out the chromatic error contributions was found, no loss of photons due in the new photo-detector and optics is designed to remove the bar thickness from the consideration, in case of the Focusing DIRC prototype and the "ultimate" DIRC. In case of the "ultimate" DIRC it is further assumed that the photon detector pixel size is so small that it does not contribute significantly to the angular error, and that the tracking contribution was reduced by installing additional local tracking near DIRC. Figure 9 shows the PID performance among various DIRC-like detectors. Of course, one never achieves a perfect performance as indicated in Fig. 9, because there are effects such as a track scattering in the bar, a combinatorial background due to ambiguities of the multiple solutions, a real particle background, overlapping events, etc., all leading to miss-ID rates. It is realistic to expect that the "ultimate" DIRC could effectively reach a π/K separation up 5-6 GeV/c at best.

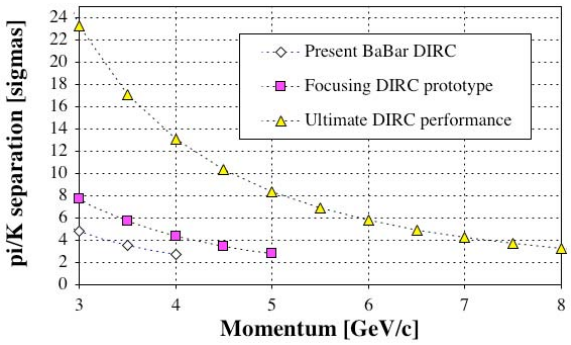

Figure 9. A π/K separation for the present BaBar DIRC (diamonds), the Focusing DIRC prototype (squares) and the "ultimate" DIRC of future (triangles).

2.3. *Ultimate DIRC design*

How would one build the "ultimate" DIRC ? Figure 10 shows two possible concepts [5]. Figure 10a shows a concept based on Hamamatsu linear MAPMT of R5900 series. It is a full 3D design with 1D pinhole (x), with a 100cm fused silica standoff, 1D lens (y), and fast timing. Given the experience with BaBar DIRC, this solution is possible to build indeed. Figure 10b shows a possible solution with wide bars for Super BaBar factory (Lum = 10^{36} $cm^{-2}sec^{-1}$). It is based on a true 3D imaging with a fast timing. The detector candidates are discussed in the following chapters.

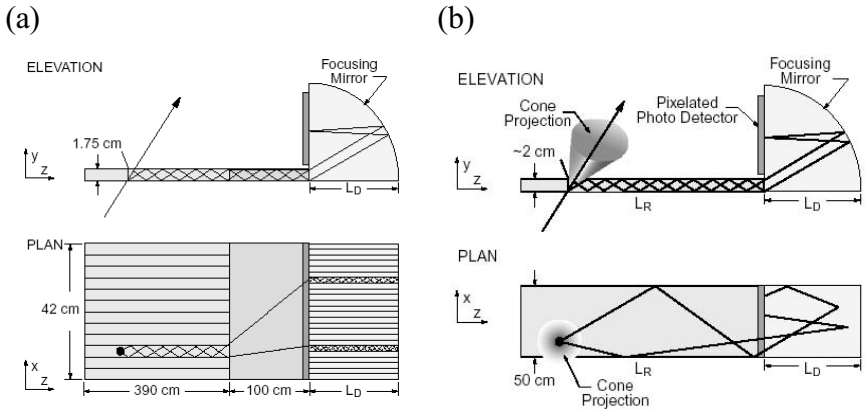

Figure 10. Possible concepts of future Focusing DIRC [5]: (a) using narrow bars, large spacer, focusing optics in a form of x-slices, each removing the bar thickness and a photon detector measuring the y-position with a ~100ps timing resolution (in this case the x-slices measure the x-coordinate), (b) using a wide Fused silica bar and focusing optics removing the bar thickness and a photon detector measuring x,y-positions with a ~100ps timing resolution per single photon.

2.4. *TOP Counter*

Nagoya group is developing the so called TOP counter, which is another variety of the DIRC-like detectors [6,7,8]. The common feature with the Focusing DIRC is the fused silica radiator, and the measurement of the time-of-propagation (TOP) of photons along the bar via the internal surface reflection. However, rather than attempting to do a 3D imaging of photons at the detector end, the Nagoya group has chosen a 2D imaging, with two basic quantities being measured: the x-coordinate (or the Φ-angle – see Fig. 11) and the TOP time with a very high accuracy (<60-70ps per single photon). Figure 11 shows two versions of the TOP counter, one with a butterfly-shaped mirror and one without it. Clearly, the second solution seems very elegant as no complicated mirror end is needed, compared to the Focusing DIRC. The Nagoya group has already demonstrated a feasibility of the TOP counter in the test beam using a multi-anode 16 channel linear array PMT, Hamamatsu R5900U-00-L16, which is not suitable for magnetic field operation though. Figure 12 shows a test beam result showing a Cherenkov ring in terms of a TOP-vs-Φ plot. This demonstrates that the TOP counter works, if the background is low. However, the 2D imaging might not work in a presence of a large background. Therefore, the Nagoya group plans to make small TOP detector segments along z-direction. That should work, but it may create non-uniformities in coverage.

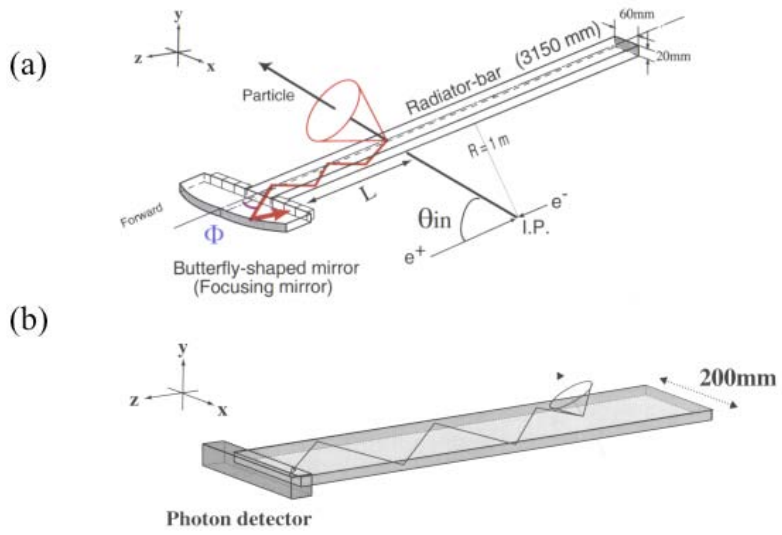

Figure 11. Two concepts of the TOP counter: (a) using a narrow Fused silica bar with a focusing mirror and a photon detector measuring the Φ angle (through x-coordinate) with a <80ps timing resolution per single photon, and (b) using a wide Fused silica bar without a focusing mirror and a photon detector measuring the photon x-positions with a <70ps timing resolution per single photon.

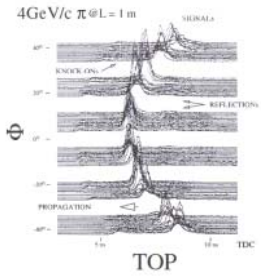

Figure 12. The 4 GeV/c test beam result showing a Cherenkov ring, in terms of TOP-vs-Φ plot, as seen in the TOP counter with the butterfly-shaped mirror.

The preferred solution of Fig. 11b is using wide bars and without a mirror. However, as the mirror is removed, the Φ vs. TOP relation cannot be uniquely extracted among many possible solutions. This ambiguity increases rapidly as one makes the bar width more narrow. Figure 13 explains this effect for the solution without the butterfly mirror. In the limit of an infinitely wide bar and infinitely wide x-measuring detector, one obtains a unique solution of the Cherenkov angle for each pair of the x-coordinate X_{true} and the TOP measurement. As one makes the bar narrower, a number of possible solutions growths. The Nagoya group has found that a bar width of 200mm is a reasonable compromise, especially, if one would segment the TOP counter in z-coordinate. Certainly, the TOP counter as shown on Fig. 11b is easier to realize in practice. For more on the photon detector choices, see Chapter 5.1.

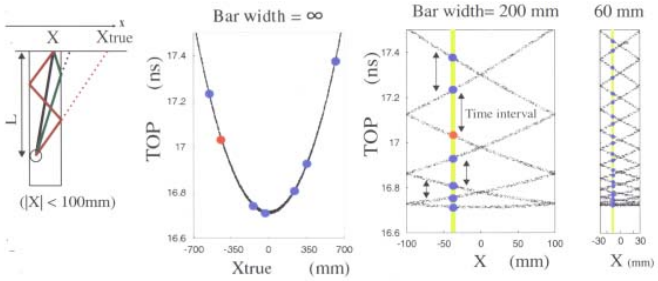

Figure 13. A graph explaining a growth of ambiguities in the TOP counter as a function of a bar width. Only for an infinitely wide bar, each photon determines the Cherenkov angle uniquely.

3. Fixed target RICH detectors

This technology is well understood. Examples of such detectors are HERA-B, HERMES, COMPASS, LHC-b and BTeV. None of this technology attempts to correct out the chromatic error. Table 2 shows a summary of their performance.

Table 2. Performance of several fixed target RICH detectors. The author's prediction [10] is based on a spreadsheet type of calculation. For a case of LHC-b, author assumed the CERN developed HPD detector.

RICH	Condition	N_o [cm^{-1}] (author)	Npe (author)	Npe (data)
ALICE	$\Theta_{inc} = 0^o$, test beam data	44	17	23
HERA-B	C_4H_{10}	45	18	19
LHC-b	Aerogel (RICH 1a)	58	26	-
LHC-b	C_4H_{10} (RICH 1b)	282	46	-
LHC-b	CF_4 (RICH 2)	174	29	-

3.1. *HERA-B*

HERA-B [9] was designed to study B and D physics in e-p collisions. Despite a very difficult radiation environment, the HERA-B RICH detector by itself was a very successful detector, which proved beyond any doubt that the Cherenkov technique can succeed even in the most harsh environment. It gave a confidence that followers such as LHC-b or BTeV will work also. HERA-B uses a C_4F_{10} gas for the radiator of 270cm length. The photon detector is based on the Hamamatsu R-5900-M16 and R5900-03-M4 multi-anode PMTs equipped with lenses to reduce the dead area effect. The photon detectors do not operate in a magnetic field. However, the interaction rates are up to 20 MHz with a beam crossing time of 96ns. Figure 14 shows a geometry of this RICH detector, as well as the predicted performance. One expects about 32 photoelectrons (30-35 actually measured) and N_o ~45cm^{-1} [10]. The limiting factor in this RICH is a poor transmission of the optics in front of the PMT.

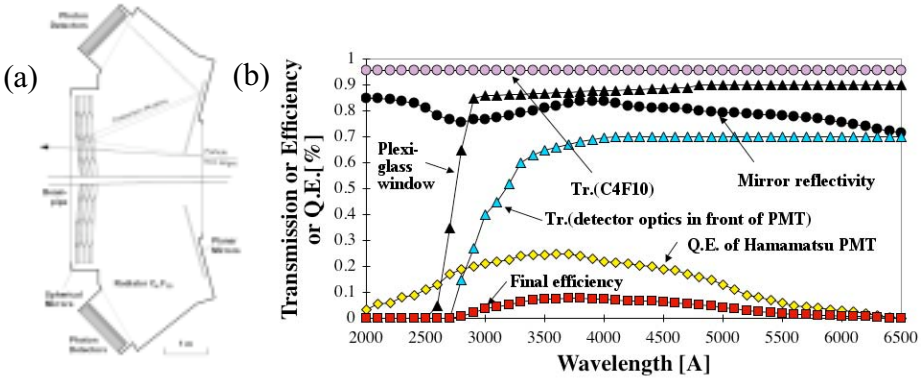

Figure 14. (a) HERA-B RICH [9]. (b) Various expected efficiencies of this detector [10].

3.2. *LHC-b*

LHC-b [11] experiment is a fixed target experiment, which will operate at LHC to study CP asymmetry in B decays. It will have two RICH detectors providing a Hadron identification between 1-65 GeV/c (RICH 1) and up to 150 GeV/c (RICH 2). To do that it needs three types of radiators: Aerogel, CF_4 and C_4F_{10} gas. The collaboration has recently chosen a DEP HPD photon detector over a 64-pad multi-anode PMT equipped with lenses. RICH detectors do not have to operate in a large magnetic field, which is a big help. However, the particle rates are enormous (up to 40 MHz per single HPD). Figure 15 shows geometries of both RICH detectors, as well as the predicted performance of the RICH 1 with a 5cm thick Aerogel radiator. One expects about 16 photoelectrons and No ~58cm^{-1} for this type of radiator [10]. Notice that in case of the Aerogel radiator what is important is a fraction of non-deflected photons rather than a simple transmission.

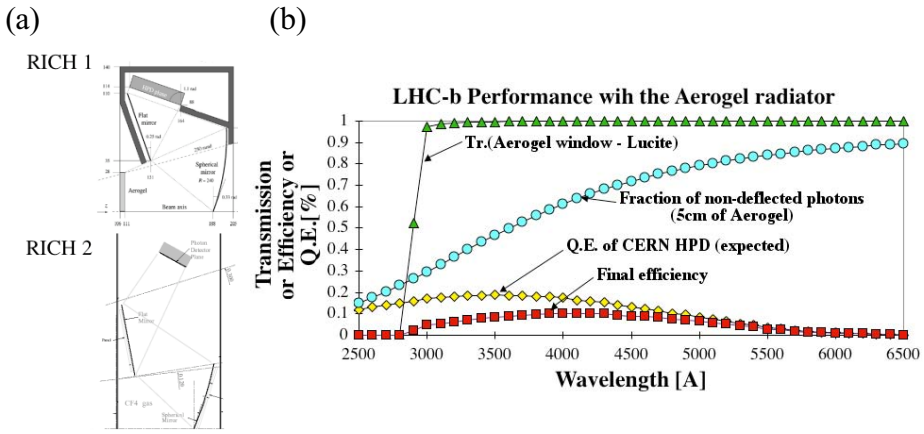

Figure 15. (a) LHC-b has two RICH detectors [11]. (b) Various efficiencies of the detector with the Aerogel radiator [10].

3.3. *BTeV*

BTeV [12] experiment is a fixed target experiment, planning to study CP asymmetry in B decays. It will have two radiators: C_5F_{12} liquid and C_4F_{10} gas. The RICH will use a DEP HPD photon detector. Figure 16 shows the geometry of the RICH detector, as well as the Cherenkov thresholds for both types of radiators.

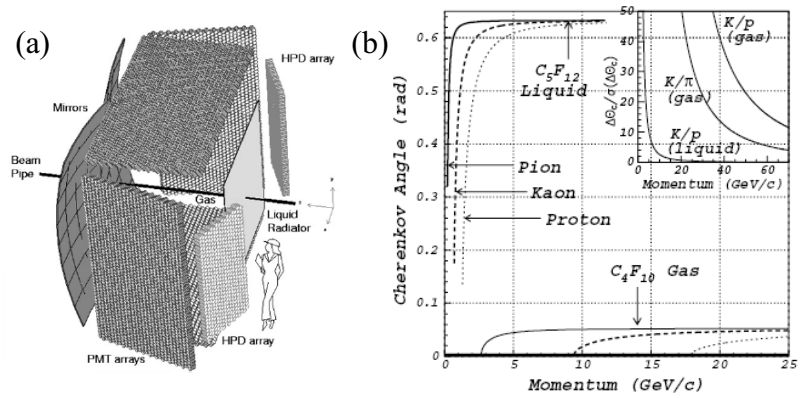

Figure 16. (a) BTeV RICH. (b) Cherenkov angle for two radiators as a function momentum [12].

4. A future 4π-geometry RICH a'la SLD CRID or DELPHI RICH ?

What if one wants to build a RICH operating in a 4π-geometry, say similar to SLD CRID or DELPHI RICH, but with a new photo-detector technology? A 4π-geometry RICH would need a very strong physics motivation because it is very hard to build. Nobody wants to repeat the TMAE-based photocathode because of aging and a necessity to heat the entire detector to 40°C. With a present know-how, I would propose a combination of DIRC to cover the low momentum PID, and a gaseous RICH to cover a high momentum range. Figure 17 shows a possible geometry. The DIRC portion, which needs to operate in the visible wavelength bandwidth to allow a good optical transmission through the fused silica bars, would be read out with the MCP-PMT photon detectors using a Bialkali photocathode. The gaseous RICH would be readout with either the Quadruple-GEM [13] or MCP-Micromegas [15] photon detectors with a CsI photocathode [14], directly evaporated on either the GEM foil or on the MCP electrode. The advantage of the MCP is that it is self-supporting, and one could do the CsI evaporation separately. The gaseous RICH detector would use a C_4F_{10} gas radiator. This portion of RICH would need to work in a UV wavelength range with all its consequences (UV mirrors, high purity gases, vessel tightness, etc.). One added bonus: DIRC would have a tracking point at the exit from a bar, which would provide an information about the track scattering, or showers.

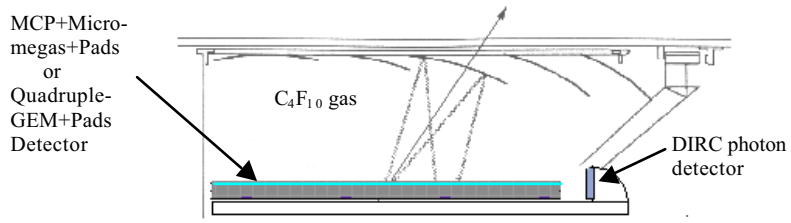

Figure 17. A possible future RICH operating in a 4π-geometry. It uses a DIRC to cover the low momentum PID range, and a gaseous RICH to cover the high momentum range. The detector for the gaseous RICH is based on either the MCP+Micromegas+Pads [15] or the Quadruple-GEM detector with a CsI photocathode [13,14].

5. Single-photon detector candidates

We will describe only Burle MCP-PMT, Hamamatsu Flat panel PMT and multi-mesh PMT detectors, which are the most advanced for the "DIRC-like" RICH applications. For more general photon detector review see [16], or for more on the HPD detectors see C. Joram's presentation [17].

One of the first decision one must make is to choose the wavelength bandwidth of a given RICH detector design. For example, in case of DIRC or Aerogel-based RICH, it is necessary to operate in the visible wavelength region, because of Fused silica's optical transmission (DIRC), or Rayleigh scattering in Aerogel radiator. Figure 18 shows author's compilation of typical photocathode candidates together with the transmission of typical RICH windows or radiator materials. For example, one can see that a Si-based photocathode would be an excellent photocathode choice to couple to the Aerogel-based RICH. However, such choice would require to build large arrays of APD detectors capable of a detection of single photons.

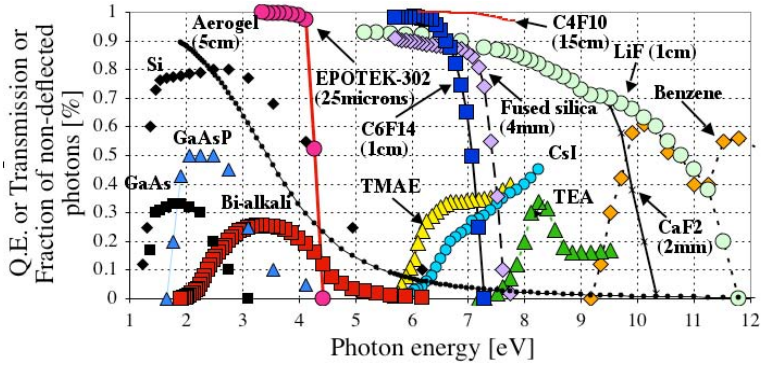

Figure 18. Quantum efficiency or transmission of various materials as a function of photon energy. In case of Aerogel, the curve represents the fraction of non-deflected photons in the radiator.

5.1. *New vacuum-based devices*

The first device we want to discuss is vacuum-based Burle 85011-501 MCP-PMT (see Fig. 19) with two micro-channel plates (MCP). Its design and measured parameter list is shown in Table 3.

Table 3. Burle 85011-501 MCP-PMT

Parameter	**Present**	**Future plan**
Photocathode type	Bialkali	Bialkali
Number of MCPs	2	2
Total average gain @ -2.4kV	~$5x10^5$	~10^6
MCP hole diameter	25μm	10μm
MCP hole angle relative to perpendicular	12^o	12^o
Geometrical collection efficiency of the 1-st MCP	60-65%	70%
Geometrical packing efficiency (raw tube)	67%	85%
Fraction of late photoelectron arrivals	~20%	-
SLAC measurement of single electron resolution (σ_{major})	54ps	-
Amplifier used in SLAC measurement	Elantec 2075C	-
Voltage gain of SLAC amplifier	130	-
Matrix of anode pixels	8 x 8	32 x 32
Number of pixels	64	1024
Pixel size	5mm x 5mm	1mm x 1mm

MCP hole diameter is 25μm at present. A new MCP with a 10μm hole size will be available soon, which would allow an operation at 1.5 Tesla. The present average gain is only ~$5x10^5$ at B = 0 Tesla, and a transit-time-distribution σ_{TTD} ~ 50-60ps at B = 0 Tesla. As one expects with all MCPs, there is a loss of primary photoelectrons due to a hole acceptance in the very first MCP, which amounts to 35-40% loss for the 25μm hole size; this will be reduced to ~30% for the 10μm hole diameter. In addition, the photons are lost due to the packing geometry due to the inefficient margins around the tube boundary. The packing fraction is ~67% for the present tube in a raw form and less than 50% for the same tube with a plastic housing; Burle Co. is aiming for ~85% for the future raw tube. In addition, some photoelectrons recoil from the very first MCP, and contribute to the tail in the timing resolution (see Fig. 19d). There may be as much as ~20% of such late photoelectrons. Combining all three losses together, even the future tube will lose ~40-45% of all primary photoelectrons due to the hole geometry, the packing fraction contributions or the late signal arrival. Such loss is very significant for any RICH applications. What does one get in return ? One gets a superior timing resolution on single photons and the operation in high magnetic field; these are attractive features, especially for the Focusing DIRC, which attempt to correct the chromatic error by timing. Figure 19c shows a single photoelectron scan across the MCP-PMT using a PiLas laser diode operating at 635nm, i.e., near the end of the Bialkali bandwidth. The scan was made using steps of 100μm in x-direction and 1mm

in y-direction. Observed uniformity of the response is about 1:1.5. Variations are caused by lower gain along the tube's edges. Figure 19d show the excellent timing resolution. The spectrum is fitted with two Gaussians. The narrow one is indicating a resolution of σ_{narrow}~54±4ps, the wide component has σ_{wide}~239±12ps. However, the spectrum has a considerable additional tail due to recoiled photoelectrons from the front surface of the MCP. This can be reduced in future tubes by reducing a gap between the photocathode and the first MCP. Burle Co. has an R&D program to reduce these tails. The PMT low gain requires a fast amplifier. We use presently a two stage amplifier based on the Elantek 2075 chip. The voltage total gain is set to 130. The amplified pulse goes to a constant fraction discriminator and a LeCroy TDC with 25ps/count [18].

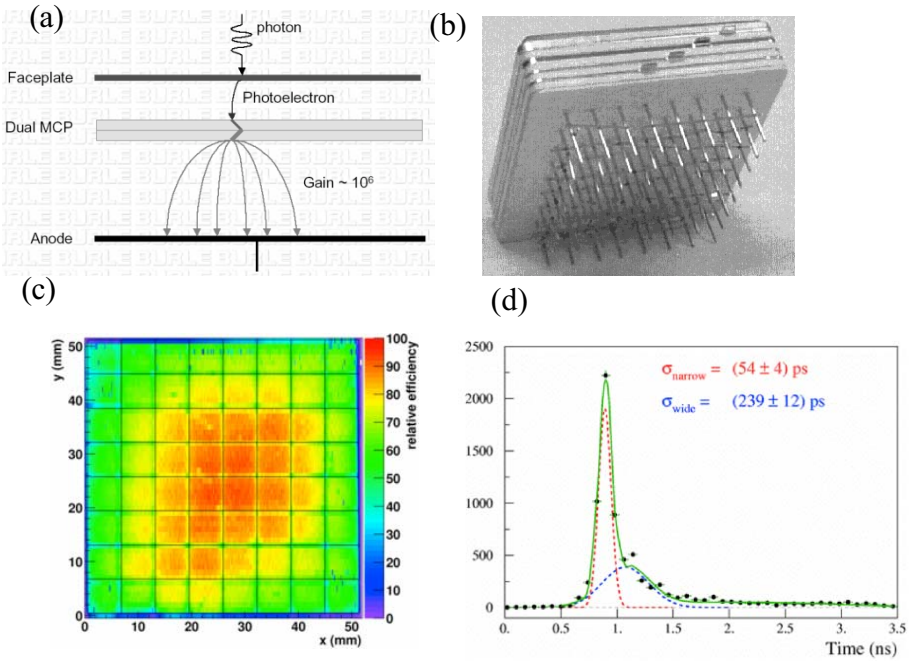

Figure 19. (a) Principle of Burle MCP-PMT with two micro-channel plates. (b) Actual MCP-PMT tube viewed from the backside. (c) Scan of the tube using the PiLas laser diode operating in single photo-electron mode at 635nm. (d) Measured single electron timing resolution of 54ps achieved in this tube. However, the distribution has a long tail due to recoil electrons [18].

The second device we want to discuss is Hamamatsu H8500 Flat Panel Multi-anode PMT, which is shown on Fig. 20. Table 4 shows its parameter list.

Table 4. Hamamatsu H8500 Flat Panel Multi-anode PMT

Parameter	Value
Photocathode type	Bialkali
Number of dynodes	12
Total average gain @ -1kV	~10^6
Geometrical collection efficiency of the 1-st dynode	70-80%
Geometrical packing efficiency	97%
Measured single electron resolution (σ_{major}) - SLAC	138ps
Fraction of late photoelectron arrivals	~5%
Matrix of anode pixels	8 x 8
Number of anode pixels	64
Pixel size	5mm x 5mm

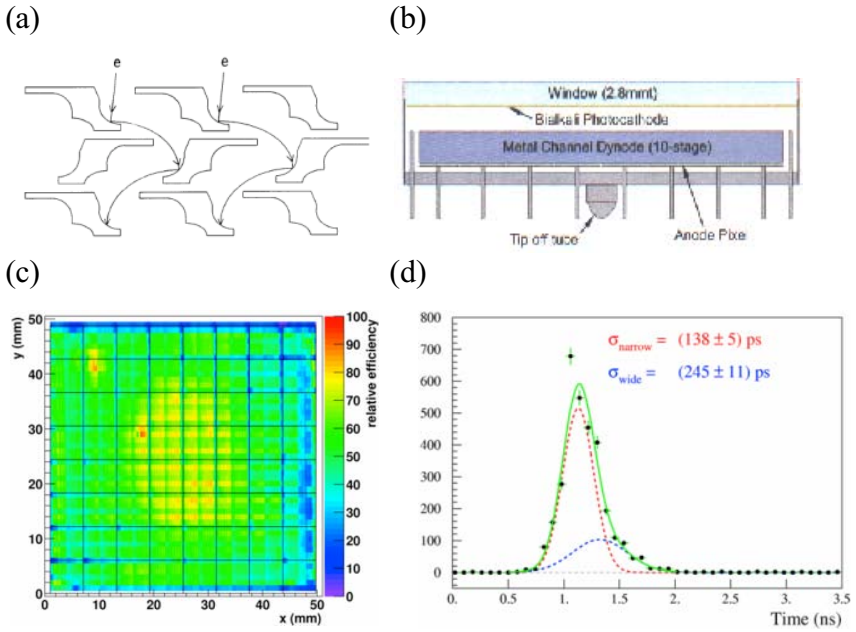

Figure 20. (a) Principle of Hamamatsu Flat Panel multi-anode H-8500 PMT. (b) H8500 tube drawing. (c) Scan of the tube using the PiLas laser diode operating in single photo-electron mode at 635nm. (d) Measured single electron timing resolution of 138ps achieved in this tube [18].

This tube cannot operate in a large magnetic field. The present average gain is only ~10^6, so the tube also needs an amplifier. There is also a loss of primary photoelectrons due to the first dynode hole acceptance , which amounts to 20-30%. In addition, the photons are lost due to the packing geometry due to the inefficient margins around the tube boundary. The packing fraction is ~97% for the present tube. A tail in the timing distribution is much smaller compared to the MCP-PMT – see Fig. 20d. Combining all three losses together, this tube loses ~25-35% of all primary photoelectrons due to the hole geometry, the

packing fraction contributions or the late signal arrival. We have measured the timing resolution of σ~140ps for single photoelectrons with the PiLas laser diode [18]. This result is worse than that of MCP-PMT, but still interesting for the Focusing DIRC to correct the chromatic error by timing.

A significant progress has also been made using a Hamamatsu multi-anode mesh R6135-L24-α,β,γ PMT, which demonstrated a transit-time-distribution of σ_{TTD} ~100ps at B = 1.0 Tesla with a photoelectron collection efficiency of 85%, and ~150ps at B = 1.5 Tesla [7,19]. This may be another avenue to build a future DIRC-like detector operating in a magnetic field of 1.5 Tesla.

5.2. *New gaseous-based devices*

It is worthwhile to mention one new concept [15]. It uses a combination of the Micromegas and the Microchannel plate (MCP) coupled to anode pads. The structure can support surprisingly large gain, which one can consider as a sign of a good concept, even though one would not wish to operate any final device at a large gain. Why we would ever consider a gaseous device now that the excellent vacuum-based devices are coming on the market ? We list several reasons:

- One could define our own geometry of the photon detector.
- Operation at very large magnetic field of 1.5 Tesla.
- A 100μm 2D positional resolution using a pad structure.

One possible application of this detector is the gaseous RICH (see chapter 4). Another application is a sealed photo-detector. However, a number of difficulties would have to be overcome for this type of application, such as:

- Bialkali photocathode operating in a permanently sealed gas envelope.
- Limit ion backflow to such a level that the gain operation is stable.

The hope is to get the PMT manufacturers interested in this idea.

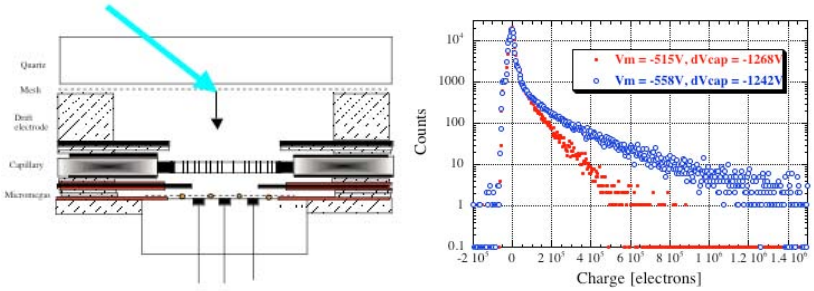

Figure 21. (a) Gaseous detector based on a "MCP+Micromegas+pads" concept. (b) A single electron pulse height spectra as a function of the Micromegas voltage Vm and the capillary (MCP) voltage dVcap obtained with 96% Ar+4% CH_4 gas [15].

5.3. *How to test a timing resolution below 100ps*

Both the Focusing DIRC and the TOP counter are pushing for a new technology of photon detectors capable of measuring a timing resolution to better than σ~100ps per single photon. This requires the development of new tools, such as light laser pulsers, fiber optics, lenses, connectors, amplifiers, discriminators, etc. For example, we have developed a good experience with a PiLas Co. laser pulser, operating at 635 or 430nm, with a time spread of FWHM ~ 35ps. To get convinced that it is really delivering such a timing stability, one needs a fast small diameter APD. Figure 22 shows an example of such tests done by the author, where a resolution of σ ~16ps was achieved with a device called SPAD diode, which is a 100μm diameter GaP APD operating in the Geiger breakdown regime [20]. This is actually a better result than what the Ref. 21 quotes, however, we have added our own constant-fraction-discriminator to their electronics. The device was operating in a single photon mode by adjusting the light amount to operate with <<1% detection efficiency. It is interesting to point out that this was achieved with a 5-meter long, 62 μm diameter, multi-mode fiber. However, one should stress that to maintain a σ =15-20ps performance is hard, as many systematic effects start playing a very significant role.

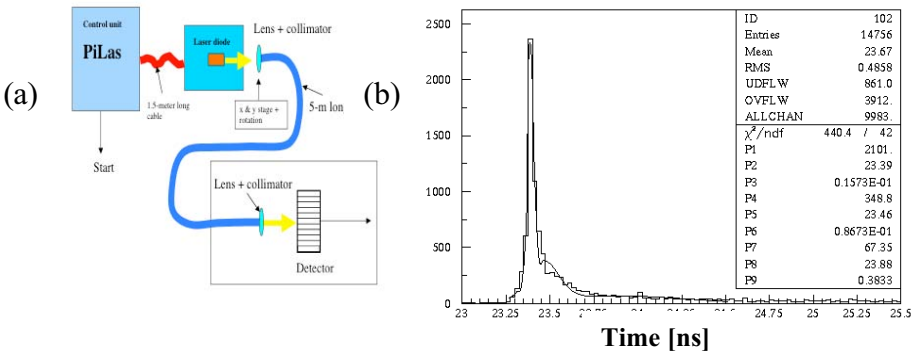

Figure 22. (a) Timing tests using the PiLas laser diode, and 5-meter long 62μm dia. Fiber equipped with lenses. (b) A resolution of σ~16ps was achieved with a SPAD detector [20] operating in the Geiger breakdown regime.

Conclusions

The Cherenkov technique is the best available method to identify Hadrons at present machines. Its future use at the Linear Collider or the Eloisatron depends on the physics one is expecting. If the chance to create quark molecules increases

with energy, there will be motivation to employ this technique as that is the only way to sort out the expected and unexpected quark states.

Acknowledgments

I would like to thank the organizer of this workshop, J. Seginot and E. Nappi, for opportunity to participate in this workshop.

References

1. B.N. Ratcliff, SLAC-PUB-8989, 2001.
2. J. Schwiening et al., Nucl. Instr.&Meth., A502(2003)67.
   J. Cohen-Tanugi, M. Convery, B. Ratcliff, X. Sarazin, J. Schweining and J. Va'vra, ICFA Instrumentation Bulletin, ICFA-J-20, Spring 2000 Issue, http://www.slac.stanford.edu/pubs/icfa/. Also as SLAC-PUB-9735, April 2003, and submitted to Nucl. Instr.&Meth.
4. G. Gratta, private communication about the KamLand experiment mineral oil; when SLAC label is added in this paper, it means that our own measurement was performed of the KamLand oil.
5. B.N. Ratcliff, Nucl. Instr.&Meth., A502(2003)211.
6. T. Ohshima, ICFA Instrumentation Bulletin, ICFA-J-20, Spring 2000 Issue, http://www.slac.stanford.edu/pubs/icfa/.
7. M. Akatsu et al, presented at RICH2002 workshop, 2002, Pylos, Greece.
8. T. Iijima, Nagoya University, SLAC Seminar, October 9, 2003.
9. J. Korpar, Nucl. Instr. &Meth., A502(2003)41.
10. J. Va'vra, Nucl. Instr.&Meth., A453(2000)262.
11. S. Easo, Nucl. Instr.&Meth., A502(2003)46.
12. S.R. Blusk, Nucl. Instr.&Meth., A502(2003)57.
13. J. Va'vra, A. Sharma, Nucl. Instr.&Meth., A478(2002)235.
14. D. Mormann et al., Nucl. Instr.&Meth., A478(2002)230.
15. J. Va'vra and T. Sumyioshi, presented at IEEE conference, October, 2003, Portland, Oregon, USA.
16. J. Va'vra, Nucl. Instr.&Meth., A502(2003)172.
17. C. Joram, Presentation at this workshop.
18. C. Field, T. Hadig, M. Jain, D.W.G.S. Leith, G. Mazaheri, B.N. Ratcliff and J. Va'vra, presented at the Instrumentation Conference on Novel detectors, May 2003, Elba, Italy, to be published in Nucl. Instr.&Meth., and also presented at IEEE, October 2003, Portland, Oregon, USA.
19. M. Hirose et al., Nucl. Instr.&Meth., A460(2001)326.
20. I. Prochazka, K. Hamal, B. Sopko, I. Macha, Microelectronics Engineering 19(1992)653, and I. Prochazka, K. Hamal, B. Greene, H. Kunimori, Optics Letters (17(1996)1375.